

# SENSITIVITY OF EQUILIBRIUM PROFILE RECONSTRUCTION TO MOTIONAL STARK EFFECT MEASUREMENTS

S.H. BATHA, F.M. LEVINTON  
Fusion Physics and Technology,  
Torrance, California

S.P. HIRSHMAN  
Oak Ridge National Laboratory,  
Oak Ridge, Tennessee

M.G. BELL, R.M. WIELAND  
Princeton Plasma Physics Laboratory,  
Princeton University, Princeton, New Jersey  
United States of America

**ABSTRACT.** The magnetic-field pitch-angle profile,  $\gamma_p(R) \equiv \tan^{-1}(B_{\text{pol}}/B_{\text{tor}})$ , is measured on TFTR using a motional Stark effect (MSE) polarimeter. Measured pitch angle profiles, along with kinetic profiles and external magnetic measurements, are used to compute a self-consistent equilibrium using the free-boundary variational moments equilibrium code VMEC. Uncertainties in the  $q$  profile due to uncertainties in  $\gamma_p(R)$ , magnetic measurements and kinetic measurements are found to be small. Subsequent uncertainties in the VMEC-calculated current density and shear profiles are also small.

## 1. INTRODUCTION

Transport, stability and equilibrium analyses of tokamak plasmas are extremely sensitive to the safety factor ( $q$ ) profile, to the value of  $q$  at the magnetic axis ( $q(0)$ ), and to the magnetic shear and current density profiles. Errors in the free-boundary equilibrium reconstruction of the internal current distribution and  $q$  profile are greatly reduced when internal poloidal field measurements are used in conjunction with external magnetics and internal kinetics measurements. Localized, internal motional Stark effect (MSE) polarimetry measurements of the poloidal field provide a better constraint for the equilibrium than do non-localized measurements provided, for example by Faraday rotation, which themselves depend on the equilibrium reconstruction. These measurements are now routinely made using MSE polarimetry on the PBX-M [1, 2], TFTR [3] and DIII-D [4] tokamaks. Although calculation of the  $q$  profile directly from the MSE measurements is possible for large aspect ratio, circular tokamaks with finite beta [5], a model of the Shafranov shift as a function of radius is required. In addition, the  $q$  profile can only be computed for part of the plasma since the MSE data do not span the entire plasma minor radius (particularly far inboard of the magnetic axis). Numerical reconstructions suffer from neither limitation and so are preferred.

A quantitative assessment of the uncertainties of the reconstructed  $q$ , shear and current profiles is required to determine the uncertainty of the analysis of transport, stability and equilibrium properties of a tokamak. Previous studies have examined the sensitivity of the reconstructed equilibrium to external measurements of the poloidal field, flux, diamagnetic flux and diamagnetic inductance [6]. The addition of poloidal magnetic field measurements inside the plasma greatly reduces uncertainty in the computed equilibria. Line integrated Faraday rotation measurements provided the first routine measurement of the poloidal field [7]. Their inclusion in reconstructions was considered by Blum et al. [8]. Lao et al. [9] estimated that the uncertainty in  $q(0)$  was reduced by a factor of 2 when two spatially localized, internal field measurements constrained the equilibrium. None of these studies directly addressed the important issue of uncertainty in the shape of the  $q$ , shear and current profiles. Equilibrium studies on the FTU tokamak found that the addition of kinetic pressure profiles to the magnetics data, without internal magnetic field measurements, could provide a reasonable estimate of the toroidal current density profile if the plasma elongation is sufficient ( $\kappa > 1.04$ ) [10].

This paper quantifies uncertainties in the  $q$ , shear and current profiles derived from measurements taken with the MSE diagnostic system on TFTR [11]

during experiments in 1992. Uncertainties for the 1993 to 1995 run are the same or are reduced slightly because of improved calibration techniques, better optical throughput and overall optimization of the entire MSE diagnostic system. The process of measuring internal pitch angles and converting to  $q$  profile information is described in Section 2. The elements of this process include the MSE polarimeter [3] itself, the TFTR external magnetics set [12], kinetic data and the VMEC free-boundary equilibrium reconstruction code [13]. The uncertainties in the  $q$  profile, central safety factor, shear profile and other computed quantities are presented in Section 3.

## 2. IMPLEMENTATION

### 2.1. Motional Stark effect polarimeter

A multichannel MSE polarimeter has been installed on TFTR and has been collecting data for several years [3, 14]. Briefly, the diagnostic technique exploits the physical phenomenon that an atom travelling across the magnetic field of a tokamak will experience a 'motional Stark effect' electric field ( $\mathbf{E}_{\text{MSE}} = \mathbf{V} \times \mathbf{B}$ ) [15]. The electric field produces Stark splitting and polarization parallel to the local magnetic field of the emitted Balmer alpha radiation when the radiation is viewed transversely to the electric field. Calibration of the polarimeter is done in two steps [14]. First, the neutral beam is injected into the torus filled with gas. The applied toroidal field is the same as that for a plasma discharge and the externally applied equilibrium field is then used to produce a known magnetic field pitch angle. The calibration includes all the effects that are present during normal plasma operation such as Faraday rotation from the window and optics, the polarization projection factor from off-normal viewing and polarization fraction effects. The second part of the calibration is a rapid radial plasma motion across the diagnostic lines of sight to cross-calibrate each channel and reduce systematic uncertainties to about  $0.2^\circ$ . The result of the calibration is that the magnetic field pitch angle,

$$\gamma_p \equiv \tan^{-1}(B_{\text{pol}}/B_{\text{tor}}) \quad (1)$$

is measured, where  $B_{\text{pol}}$  is the poloidal field and  $B_{\text{tor}}$  is the toroidal field.

On TFTR, the pitch angle is measured at twelve locations along the equatorial midplane of the tokamak. The measurement volume is limited to the intersection of the collection optics line of sight and the

neutral beam path resulting in a radial resolution of about 3 cm. The line of sight to line of sight spacing is known to an accuracy of better than  $\pm 0.2$  cm with an absolute uncertainty in the line of sight major radius of  $\pm 0.8$  cm. In 1992, 10 lines of sight were available. For the 1993 to 1995 series of experiments using deuterium and tritium as fuel, two additional lines of sight were added for a total of 12. The lines of sight span the major radius interval  $R_{\text{mag}} - 0.3a < R < R_{\text{mag}} + a$  along the equatorial midplane, where  $R_{\text{mag}}$  and  $a$  are the magnetic axis and minor radius of the plasma, respectively.

Typical total uncertainties in the MSE pitch angles are shown in Fig. 1 for both 1992 and 1993 to 1995 data. Statistical uncertainties are estimated directly from the raw data during analysis of each discharge.

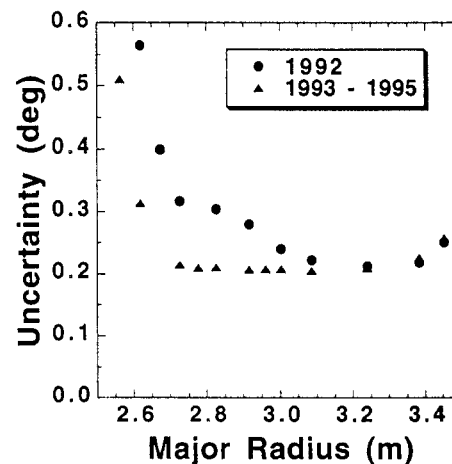


FIG. 1. Total (systematic and statistical) uncertainty of the MSE-measured pitch angle data for 1992 (closed circles) and for 1993 to 1995 (closed triangles). The data were averaged over a 20 ms interval.

The pitch angles are usually averaged over a time bin of 3 to 50 ms although the data are collected at 2000 samples per second. The statistical uncertainties are insensitive to the averaging interval for averaging intervals greater than 20 ms and increase by only about 50% for shorter averaging times [14]. Added, in quadrature, to the statistical uncertainties are estimates of the systematic uncertainties (typically  $0.2^\circ$ ) obtained from the plasma motion calibration discussed in Ref. [14]. The uncertainties are greatest at the most inboard lines of sight because of vignetting of the collection optics and beam attenuation. The uncertainties also rise at the outboard edge owing to lower plasma density.

## 2.2. TFTR magnetic diagnostics

The standard set of TFTR magnetic diagnostics [12] is employed during the equilibrium reconstruction using VMEC. These include diamagnetic flux, plasma current, saddle coil and 25  $B_\theta/B_\rho$  magnetic loop measurements. Each of these measurements is made outside of the vacuum vessel. Additionally, the values of the currents circulating through the external (toroidal, poloidal, etc.) magnets are required in order to determine the vacuum magnetic field. A summary of the quantities used and their errors is given in Table I. The uncertainties are predominantly sys-

TABLE I. ESTIMATES OF UNCERTAINTIES FOR EXTERNAL MAGNETICS MEASUREMENTS

Quantity	Symbol	Uncertainty	Units
Diamagnetic flux	$\phi_{\text{diam}}$	$\pm 1$ mWb	Wb
Plasma current	$I_p$	$\pm 0.7\%$	MA
External coil currents		$\pm 0.5\%$	kA
Saddle coils		$\pm 30$ mWb	Wb
$B_\theta/B_\rho$ loops		5% typical	T

tematic, arising from uncertainties in absolute sensor calibrations, from residual uncompensated coupling of the measurements to the toroidal field and local eddy currents, and from uncertainties in the absolute positions and dimensions of the pick-up loops themselves. A 5 ms averaging window was typically used to sample the magnetic data, which were digitized at a 2 kHz rate. With this averaging window, the noise levels on the data were substantially less than the systematic uncertainties.

## 2.3. Equilibrium reconstruction with VMEC

The plasma equilibrium at a single time point is reconstructed from the MSE pitch angle data, the external magnetics measurements, and total thermal pressure, including the numerically computed fast-ion beam pressure [16] using the free-boundary variational moments equilibrium code (VMEC) [13]. The VMEC code solves the MHD equilibrium equation,  $\mathbf{J} \times \mathbf{B} = \nabla p$ , in inverse co-ordinates using a steepest descent algorithm to minimize the ideal MHD energy. An inverse co-ordinate representation determines the mapping of the cylindrical co-ordinates ( $R, Z$ ) in terms of the flux co-ordinates ( $\Phi, \theta$ ). Here,  $\Phi$  is the toroidal flux and  $\theta$  is the poloidal angle. The MHD energy minimization is performed for prescribed pres-

TABLE II. NORMALIZED RMS DEVIATION BETWEEN THE EQUILIBRIUM-CALCULATED VALUES AND EITHER THE MEASURED OR THE BENCHMARK CASE 1, SHOWING THE SENSITIVITY OF VMEC RECONSTRUCTIONS USING VARIOUS COMBINATIONS OF PERTURBED INPUT DATA

(Case 1, experimental data; cases 1(a) and (b), different plasma boundary guesses and reconstructed data; case 2, no  $B_\theta/B_\rho$  loops used in case 1 reconstruction; case 3, no saddle coils used in case 1 reconstruction; case 4, neither  $B_\theta/B_\rho$  loops nor saddle coils used in case 1 reconstruction. NF denotes no fit in this case.)

Shot	Case	Type	RMS Pressure	RMS MSE	RMS $B_\theta/B_\rho$	RMS saddle	$\Delta\phi_{\text{diam}}$ (mWb)
65 610	1	Benchmark	0.017	0.025	0.035	0.033	0.823
	1(a)	Vary initial conditions	0.010	0.004	0.007	0.013	0.166
	1(b)	Vary initial conditions	0.011	0.005	0.005	0.004	0.187
	2	Benchmark, no $B_\theta/B_\rho$	0.017	0.023	NF	0.028	0.800
	3	Benchmark, no saddle	0.017	0.028	0.035	NF	0.879
	4	Benchmark, no $B_\theta/B_\rho$ or saddle	0.017	0.021	NF	NF	0.940
68 257	1	Benchmark	0.019	0.044	0.037	0.042	1.695
	1(a)	Vary initial conditions	0.008	0.011	0.006	0.002	-0.127
	1(b)	Vary initial conditions	0.009	0.012	0.006	0.004	-0.072
	2	Benchmark, no $B_\theta/B_\rho$	0.020	0.041	NF	0.035	1.794
	3	Benchmark, no saddle	0.020	0.043	0.038	NF	1.768
	4	Benchmark, no $B_\theta/B_\rho$ or saddle	0.020	0.041	NF	NF	1.910

sure ( $p$ ) and  $q$  profiles. To match these profiles to internal kinetics and magnetics data (including MSE data), a second minimization of the data mismatch  $\chi^2$  is performed simultaneously with the primary MHD minimization. Thus, the steady state solution to this iterative procedure yields a result that satisfies the equilibrium equations with  $p(\Phi)$  and  $q(\Phi)$  profiles to minimize  $\chi^2$ .

Cubic tension splines are used to represent  $p$  and  $q$ , with the knot locations for  $q$  redistributed in  $\sqrt{\Phi}$  space, which gives the most non-redundant information [13]. The knot values, but not the knot locations, are allowed to vary during the MHD energy minimization to obtain a minimum for  $\chi^2$ . It was found that varying the tension parameter in the  $q$  cubic spline changed the reconstructed  $q$  profile by less than the uncertainty quoted in this paper. However, the magnetic shear changed by more than the uncertainty quoted if the tension was reduced by more than a factor of 10 from the usual value. The situation may be different for non-monotonic  $q$  profiles where there is inherently more structure in the  $q$  profile.

A typical VMEC equilibrium for TFTR matches up to 91 measurements of plasma properties, such as the plasma current, diamagnetic flux, 6 saddle coils, 25  $B_\theta$  loops, 25  $B_\rho$  loops, 21 pressure points and 12 MSE data values. Not all of these measurements are independent, however. The TFTR plasma is nearly symmetric in the vertical direction, i.e. the differences in the magnetics measurements at  $(R, Z)$  and  $(R, -Z)$  are always less than the uncertainty of the measurement. Consequently, half the saddle coils and magnetic field loops are redundant. The total number of independent measurements,  $N$ , is 63. A 'good' fit typically has a value of  $\chi^2$  less than 50, so that  $\chi^2/N < 1$ .

In addition to the standard magnetics information of currents and diamagnetic flux, the code requires, as a minimum, the MSE pitch angle profile and the pressure profile. Usually, the pressure profile is provided by the time dependent interpretive transport code TRANSP [17], where the measured ion and electron thermal pressures are combined with the fast-ion beam pressure. The uncertainty in the pressure profile was estimated by performing a series of 30 TRANSP runs with differing numbers of Monte Carlo particles and with the density, visible bremsstrahlung and electron temperature experimental measurements varied within their uncertainties. It was found that the computed pressure varied by about 6% except near the centre and edge of the plasma where the variations were up to 12 and 40%, respectively. Variations at

the centre of the plasma are assumed to be due to the finite number of Monte Carlo particles used to model the slowing down and deposition of the neutral beam particles [16]. Edge variations are attributed to measurement errors associated with low densities.

The sensitivity of VMEC to different combinations of experimental data and to small displacements in its initial starting point has also been tested. Sensitivity to the initial starting point was tested by reconstructing two typical TFTR discharges using all the available experimental data. Then the reconstructed physical data were used as input data for further reconstructions. In this way, a set of input data for which the equilibrium solution is known was generated. This set was then used as a benchmark to compare against other perturbative numerical experiments which are described below.

Table II presents the results of these experiments by showing the normalized root-mean-squared deviation of the reconstructed data from the benchmark data:  $\text{RMS } X \equiv [(X_{\text{rec}}^2 - X_{\text{ben}}^2)/X_{\text{ben}}^2]^{1/2}$ , where  $X_{\text{rec}}$  is the reconstructed data and  $X_{\text{ben}}$  is the benchmark result (case 1), which uses actual experimental data. Shown are the normalized RMS differences for the pressure profile (RMS pressure), the MSE profile (RMS MSE), the  $B_\theta/B_\rho$  loop data set (RMS  $B_\theta/B_\rho$ ) and the saddle coil data set (RMS saddle). The difference between the benchmark and computed diamagnetic flux is tabulated as  $\Delta\phi_{\text{diam}} \equiv (\phi_{\text{diam}}^{\text{rec}} - \phi_{\text{diam}}^{\text{ben}})$ .

Case 1 is the original benchmark reconstruction using actual experimental data. Cases 1(a) and (b) use the reconstructed data from case 1 as input data

TABLE III. UNCERTAINTIES OF VARIOUS CALCULATED QUANTITIES (AVERAGED OVER 12 DISCHARGES)

Quantity	Symbol	Standard deviation	Units
Magnetic axis	$R_{\text{mag}}$	1.6	cm
Geometric axis	$R_{\text{geo}}$	2.1	cm
Stored energy	$W$	9%	MJ
Difference in diamagnetic flux (measured-calculated)	$\Delta\phi_{\text{diam}}$	1.7	mWb
Internal inductance	$\ell_i$	11%	
Diamagnetic energy	$\mu_i$	0.08	
Safety factor	$q(0)$	6%	
Edge $q$	$q(a)$	11%	
Volume	$V$	6%	$\text{m}^3$

testing the sensitivity of VMEC to different initial guesses for the plasma boundary. In principle, the cases 1(a) and (b) normalized RMS differences should be uniformly zero. The extent to which they are not represents the baseline noise level of the VMEC minimization procedure.

The sensitivity of VMEC to the magnetic data was examined in cases 2 to 4 by using the original experimental data and including or excluding some of the magnetic data sets. Cases 2 and 3 represent the elimination of either the  $B_\theta/B_\rho$  loops or the saddle coils, respectively, from the case 1 data set. In case 4, both data sets are removed. For both shots, the RMS saddle and RMS MSE improve very slightly when the  $B_\theta/B_\rho$  loops are removed. Conversely, when the saddle loops are removed, the RMS MSE increases. In both cases,  $\Delta\phi_{\text{diam}}$  either stays the same or degrades. When both magnetic data sets are removed, the RMS MSE again improves slightly, but  $\Delta\phi_{\text{diam}}$  degrades. These observations and the observation that no RMS difference value decreases significantly as a result of excluding subsets of the data, rule out the possibility that any subset of the magnetic data is inconsistent within a statistical variation.

A sensitivity study was also conducted where the values of the external coil currents, which determine the vacuum field inside the torus, were perturbed by 1%, which is twice the experimental uncertainty. No sensitivity to these perturbations was observed.

### 3. UNCERTAINTY ANALYSIS

Uncertainty analysis of equilibrium scalar quantities such as  $q(0)$  as well as profile quantities such as  $q$ , current density and shear, has been performed using VMEC. For each discharge studied, the original data file was replicated a few hundred times with the experimental data varied by a Gaussian distribution having a standard deviation equal to the uncertainty in the measurement. Equilibria were then reconstructed on each perturbed data file using VMEC and the resulting values of many plasma parameters were tabulated. The results of 1000 reconstructions from a single discharge with  $I_p = 1.4$  MA (discharge 68 257 at 4.20 s, data averaged over 20 ms) are shown in Figs 2 to 8. The results from a series of 12 neutral beam heated discharges (200 reconstructions per discharge) are given in Table III. These 12 discharges spanned a wide range of operational regimes on TFTR. For example, the plasma current

was between 0.5 and 2.0 MA, the neutral beam power varied between 10 and 23 MW, the diamagnetic flux was between  $-1$  and 40 mWb,  $0.4 < \beta_{\text{pol}} < 2$ , the central density,  $n_e(0)$ , was between  $2.5 \times 10^{13}$  and  $5.3 \times 10^{13} \text{ cm}^{-3}$ , and the density peaking factor,  $n_e(0)/\langle n_e \rangle$ , was between 1.5 and 3.0. All  $q$  profiles considered were monotonic, i.e. there were no regions of reverse magnetic shear present. The uncertainty, defined to be the standard deviation, of each measurement was computed for each discharge. The average standard deviation of the twelve discharges for each measurement is presented in Table III. None of the discharges deviated significantly from the averages shown in Table III.

An important parameter obtained from the equilibrium reconstruction is  $q(0)$ . Figure 2 demonstrates that this measurement is very robust, having a standard deviation of 5.2% for discharge 68 257. This discharge was heated with 17.6 MW of neutral beam power, had an  $H$  factor of about 2 and did not have sawtooth oscillations. This discharge satisfied the  $\omega^*$  stabilization criterion for sawtooth suppression with  $q(0) < 1$  [18]. Table III shows that the average uncertainty of  $q(0)$  measured by MSE in the ensemble of discharges is 6%. The impact of statistical, and to some extent systematic, uncertainty in the measurements is reduced because VMEC uses a global fit to all of the poloidal field measurements, effectively averaging over several MSE measurements. A value of  $q(0)$  10% less than the equilibrium reconstruction value was found using a direct analytic calculation. This illustrates the improved accuracy and smoothing available from the full reconstruction.

The determination of the diamagnetic flux is not as robust, however. Figure 3 shows that the average difference between the measured and calculated diamagnetic flux is almost  $-1.0$  mWb, at the accuracy of the magnetic measurement (see Table I). The standard deviation is 1.7 mWb, nearly twice the accuracy of the measurement. This difficulty in matching the magnetics measurement is typical of the data examined in this study, see Table III. The difficulty in matching the diamagnetic flux measurement is not understood, although systematic uncertainties in the flux measurement do not seem to be the cause of this problem. The diamagnetic measurement affects primarily the  $q$  profile in the outer half of the plasma, which indicates a disagreement between the MSE data in this region and the flux measurement. The positions of the geometric and magnetic axes are resolved to an uncertainty of  $\pm 2.0$  and  $\pm 1.3$  cm, respectively, as demonstrated in Fig. 4.

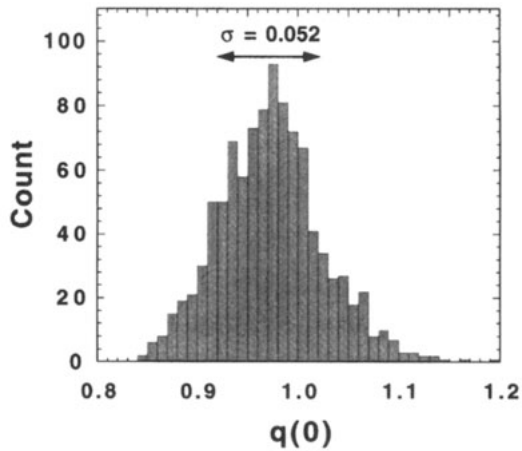


FIG. 2. Distribution of the calculated  $q(0)$  for discharge 68257. The value of  $q(0)$  determined from the experimental data was 0.966. With an ensemble of 1000 equilibria reconstructed by VMEC, where each experimental datum was perturbed by its uncertainty, the average value of  $q(0)$  was calculated to be 0.973 with a standard deviation of 5.2%. A direct analytic calculation from the polarimeter data gave  $q(0) = 0.86$ .

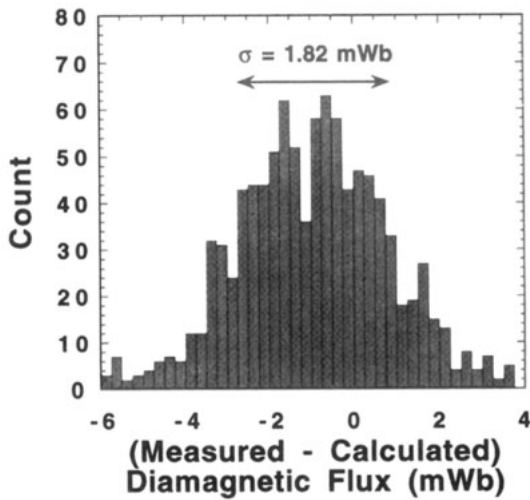


FIG. 3. Distribution of the difference between the measured and calculated diamagnetic flux,  $\Delta\phi_{diam}$ , for discharge 68257. An ensemble of 1000 equilibria reconstructed by VMEC, where each experimental datum was perturbed by its uncertainty, calculated the average value of  $\Delta\phi_{diam}$  to be  $-1.00 \text{ mWb}$  with a standard deviation of  $1.82 \text{ mWb}$ .

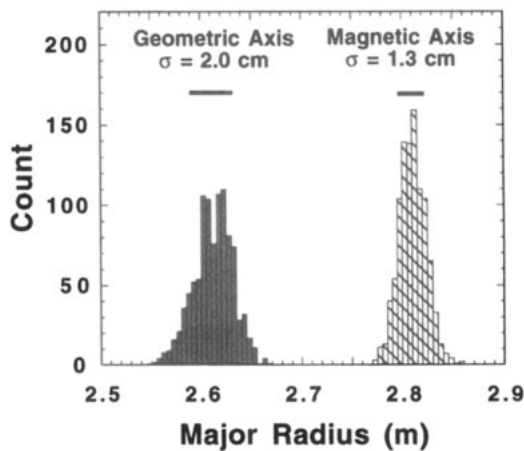


FIG. 4. Distribution of the calculated values of the geometric ( $R_{geo}$ ) and magnetic ( $R_{mag}$ ) axes for discharge 68257 at 4.2 s. The baseline value of  $R_{geo}$  was 261.1 cm while an ensemble of 1000 equilibria reconstructed by VMEC, with each experimental datum perturbed by its uncertainty, calculated the average  $R_{geo}$  to be 261.2 cm with a standard deviation of 2.0 cm. The baseline value of  $R_{mag}$  was 281.4 cm while the average  $R_{mag}$  was 281.0 cm with a standard deviation of 1.3 cm. The bold lines show twice the standard deviation.

To determine the dominant sources of uncertainty, the sensitivity of the reconstruction to the uncertainty of subsets of the experimental data was examined. An important parameter is the diamagnetic flux,  $\phi_{\text{diam}}$ , which has been used in some cases to improve the stability of the solution in circular geometry [19] and to compute separately the values of  $\beta_{\text{pol}}$  and the internal inductance ( $\ell_1$ ) from Shafranov surface integrals [20]. It was found for the TFTR plasmas considered here that the input value of the diamagnetic flux was an unimportant measurement for determining global plasma parameters. Changes in any of the computed quantities were less than 2% when the input value of  $\phi_{\text{diam}}$  was varied by  $\pm 4$  mWb, where typical values of  $\phi_{\text{diam}}$  are between  $-1$  and  $40$  mWb.

The edge toroidal flux,  $\phi_{\text{tor}}$ , has a stronger effect, but only on the plasma volume and related quantities, such as the geometric axis, surface area and stored energy. In Fig. 5, the results of a study where the input value of the edge flux was varied by  $\pm 4$  Wb are shown. It is readily apparent that  $q(0)$  and  $R_{\text{mag}}$  are unaffected but that the position of the geometric axis varies by  $\pm 6$  cm from the nominal value of  $2.61$  m over this range of flux. The VMEC equilibria reported in this paper used the value of  $\phi_{\text{tor}}$  calculated by a

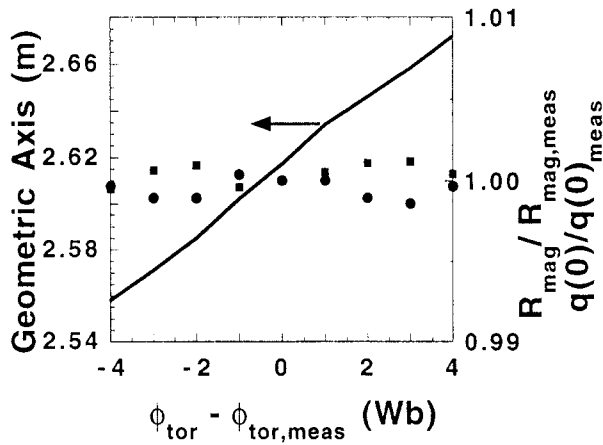


FIG. 5. Equilibrium for discharge 68257 at 4.2 s computed several times with different values of the edge toroidal flux. The major difference is the position of the geometric axis of the plasma and related quantities such as plasma volume, stored energy and internal inductance. The position of the magnetic axis (closed circles) and the value of  $q(0)$  (closed squares), shown normalized to their values at the measured value of the flux, are not sensitive to variations in the flux.

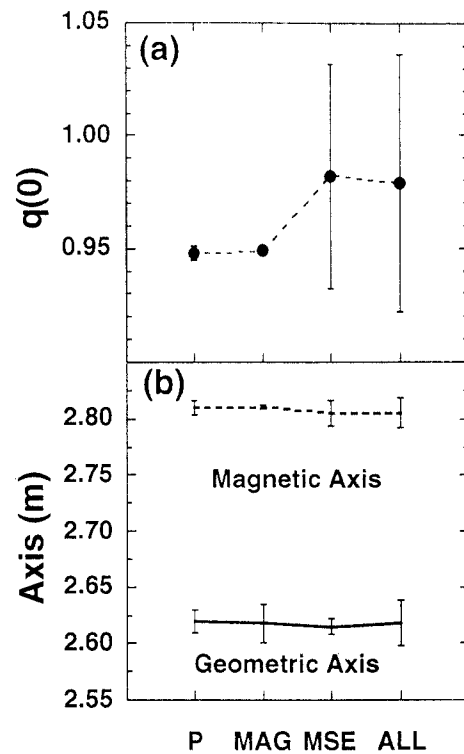


FIG. 6. Average value and uncertainty of (a)  $q(0)$  and (b) the magnetic and geometric axis locations when subsets of the experimental data from a single discharge were varied while all the other measurements were held at their measured values. The varied quantities were the pressure data (P), all of the magnetics data including coil currents and flux measurements (MAG), and the MSE measurements including systematic uncertainties of pitch angle and radial location (MSE). Also included is the result when all of the measured quantities were varied within their uncertainties (ALL).

current filament model [21] and no constraints were put on the size of the plasma by the position of the limiters. It is worth noting that each of the computed equilibria in Fig. 5 are equally good. That is, the value of  $\chi^2/N$  is approximately the same and is less than 1 for each value of the edge toroidal flux, no matter how far from the value determined by the current filament analysis.

A further set of studies was performed where subsets of the experimental data were varied according to their uncertainty, as above, but the rest of the experimental data were held fixed at their measured values. Three data subsets were varied: the pressure data, the magnetics data including all coil currents and flux measurements, and the MSE data. Figure 6(a) shows

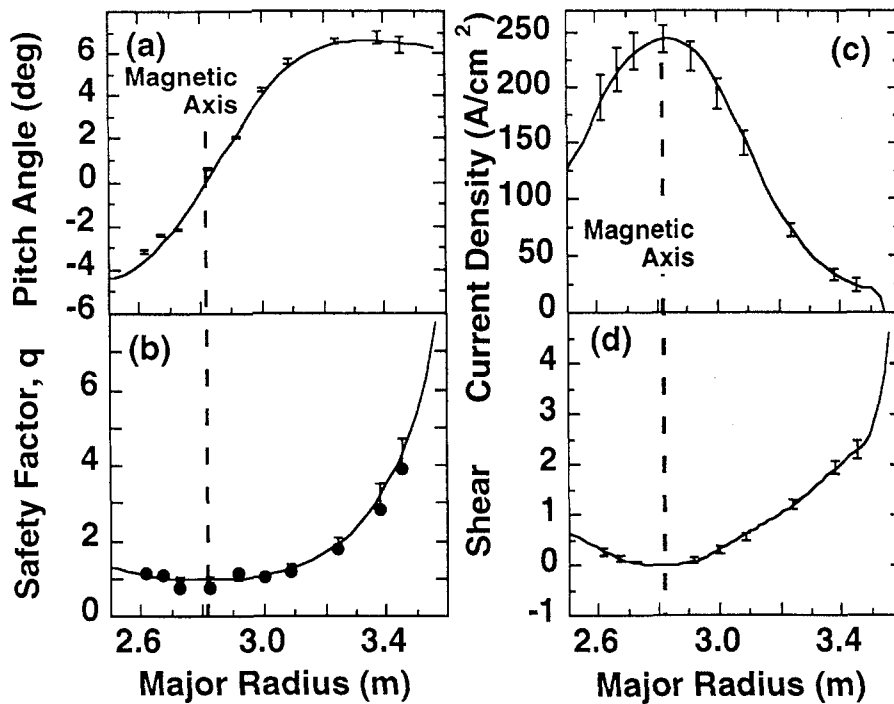


FIG. 7. Computed baseline (a) pitch angle profile and MSE measurements (at the centre of the error bars), (b)  $q(R)$  profile, (c) current density profile and (d) shear profile for discharge 68257. The error bars represent the standard deviation calculated from an ensemble of 1000 equilibria reconstructed by VMEC, where each experimental datum (MSE, magnetics and pressure) was perturbed within its uncertainty. Also shown in (b) is the  $q$  profile (full circles) computed by an analytic expression for  $q(R)$  [5].

that the dominant contributors to the uncertainty in  $q(0)$  are the MSE measurements. The pressure and magnetics data alone would lead to a different value of  $q(0)$ , but have little effect on the uncertainty of  $q(0)$  when MSE data of sufficient spatial resolution are also present. The increase in  $q(0)$  when only the MSE data were varied is due to the different relative uncertainties of the MSE data points on each side of the magnetic axis which dominate the determination of  $q(0)$ . These results are consistent with previous studies done with simulated data [8, 9].

The positions of the magnetic and geometric axes are sensitive to all three subsets of the data, Fig. 6(b). The magnetic axis is relatively insensitive to the magnetics data, but responds to the uncertainty in the pressure and MSE data. The MSE data can independently determine the location of the magnetic axis since the axis is located at the position where the pitch angle is zero since all MSE measurements in TFTR are made along  $Z = 0$ . Similarly, the peak of the pressure profile can determine the location of the

axis, assuming that the plasma rotation is small. The geometric axis does not respond to the MSE data, but does respond to the uncertainty in the pressure and magnetics data. The dependence on the magnetics data was also seen in Fig. 5. The pressure data affect the geometric axis position because the pressure profile includes an implicit measurement of the plasma minor radius given by the peak and edge pressure locations.

Important information for stability and transport analyses is provided by the profiles of  $q$ , the current density  $j$  and the shear. The profiles are calculated along the midplane of the plasma, which is assumed to be the plane of vertical (up-down) symmetry. Figure 7(a) displays the measured and calculated pitch angle profiles for discharge 68257. The baseline  $q$  profile is shown in Fig. 7(b), where the error bars represent the standard deviation of the computed  $q$  values at the radial locations of the MSE measurements when all of the experimental data (MSE, external magnetics and pressure) are varied within

their experimental uncertainty. The standard deviations can be as little as 5% of the  $q$  value near the centre of the plasma, increasing to  $\approx 10\%$  near the edge of the plasma. The analytic calculation of  $q$  directly from the MSE data [5] is also shown in Fig. 7(b). The calculation covers only a subset of the plasma major radius and does not correctly calculate the magnetic shear. None of the discharges considered in this study had sawteeth. When coherent magnetohydrodynamic modes are present, the calculated location of the rational surface agrees with the measured inversion radius to within the uncertainties of the equilibrium reconstruction and the inversion radius measurement [14].

Similar displays of the current density and shear profiles are shown in Figs 7(c) and (d), respectively. The shear is defined as [22]

$$\text{Shear} = \frac{2V}{q} \frac{\partial q}{\partial \psi} \frac{\partial \psi}{\partial V} \quad (2)$$

where  $V$  is the plasma volume and  $\psi$  is the poloidal flux. This definition of shear reduces to the more common  $(r/q)\partial q/\partial r$  for a circular plasma in the limit of large aspect ratio. The uncertainty in the  $j$  profile is small, of the order of 10%, but increasing slightly at the edge where the current is small. The uncertainty in the shear profile is also small, being less than  $\pm 0.15$  for  $r < 0.8a$ . These uncertainties are the same, whether the analysis is performed at constant major radius, as shown in Fig. 7, or at constant toroidal flux.

The sensitivity of the  $q$  and shear profiles at  $r \approx a/4$  to the uncertainty in subsets of the data is displayed in Fig. 8. In Fig. 8(a), the value of  $q$  at  $R = 3.00$  m is more sensitive to the uncertainties in the pressure and magnetics data than is  $q(0)$ , given in Fig. 6(a). The uncertainty in the MSE data is the dominant source of uncertainty for  $q(R)$ . Inclusion of the MSE data is essential: without this information, the code would consistently determine a value of  $q(R = 3.00$  m) that is too small. The pressure profile is an important source of uncertainty for the shear at  $R = 3.00$  m, Fig. 8(b), contributing about half as much uncertainty as the MSE measurements.

The uncertainty in the MSE data affects the shapes of the calculated profiles as well as the scalar quantities shown in Fig. 8. Recall that all three of these quantities are the results of the equilibrium reconstruction, not prescribed parameters. The pressure and magnetics data subsets cause the magni-

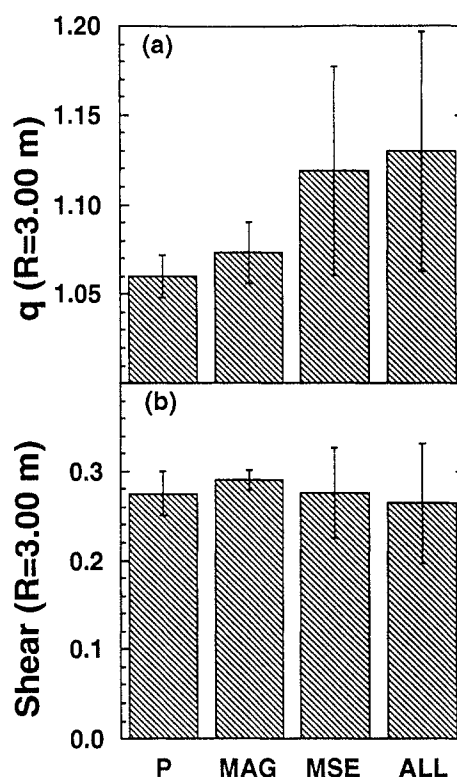


FIG. 8. Value and uncertainty of (a)  $q$  and (b) shear at a major radius of 3.00 m when subsets of the experimental data were varied while all other measurements were held at their measured values. The varied quantities were the pressure data (P), all of the magnetics data including coil currents and flux measurements (MAG), and the MSE measurements including systematic uncertainties of pitch angle and radial location (MSE). Also included is the result when all of the measured quantities were varied within their uncertainties (ALL).

tudes of  $q$  and shear to vary over about a quarter the range shown in the figures. As shown in Fig. 6, the value of  $q(0)$  does not vary. The MSE data, however, cause almost all of the variation in  $q$ , shear and  $q(0)$ . The relationship among these three quantities is apparent. The value of the shear decreases because the edge value of  $q$  is fixed while  $q(0)$  is increasing, leading to a 'flatter' profile (lower shear) in the centre of the plasma.

#### 4. DISCUSSION AND CONCLUSION

This analysis has concentrated on several TFTR discharges with  $0.75 < q(0) < 2.3$ . A more demanding test of the diagnostic system is to examine discharges that deviate significantly from the standard

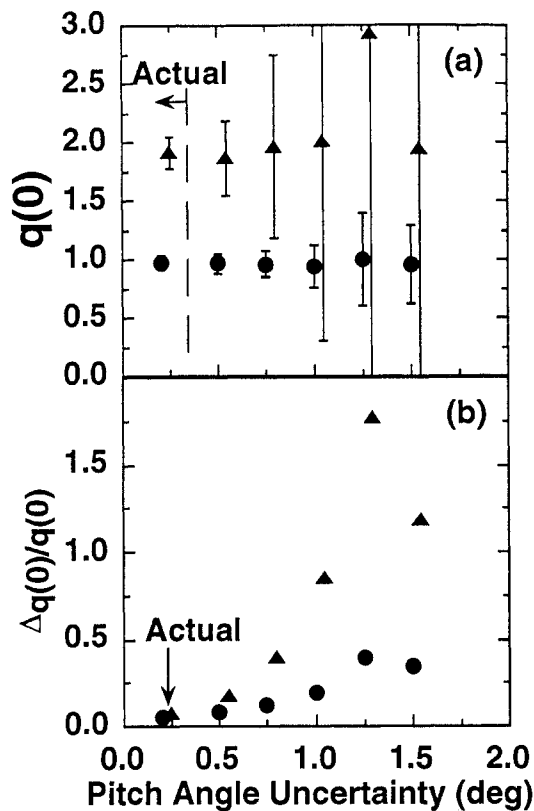


FIG. 9. The value (a) of  $q(0)$  varies and the uncertainty (b) of  $q(0)$  increases dramatically as the uncertainty in the measurement of the magnetic field pitch angles increases. The effects are shown for a typical supershot discharge, 68 257 (closed circles) and a discharge with high  $\beta_{pol}$ , 69 217 (closed triangles). The data for discharge 69 217 have been shifted in uncertainty by  $+0.05^\circ$  to avoid overlapping with the other data. The points labelled 'actual' used the uncertainties shown in Fig. 1. The error bars represent the standard deviation calculated from an ensemble of 200 equilibria reconstructed by VMEC, where each experimental datum was perturbed within its uncertainty.

operational space of TFTR. Such discharges include high  $\beta_{pol}$  regimes achieved through current ramping [23] as well as rotating plasmas [14]. Great difficulty in matching the external magnetic loops and saddle coils has been encountered for high- $\beta_{pol}$  discharges where the plasma developed a separatrix as opposed to being a limited plasma [23]. This is speculated to be due to currents outside the separatrix. The main difficulty is in matching the external magnetic loops and saddle coils. This remains an active area of research. In addition, the effects of plasma rotation and the distinction between parallel and perpendicular pressure [24] may help to mitigate the difference between the computed and observed measurements.

Neither of these physical effects are included in the present data matching version of VMEC.

A great deal of effort has been expended to provide an accurate calibration of the MSE pitch angle measurement and to reduce the uncertainty in the measurement from  $0.5$  to  $0.2^\circ$  [14]. Figure 9 shows that the uncertainty in the value of  $q(0)$  is dependent on the uncertainty assigned to the MSE pitch angle data. For each data point in Fig. 9, the uncertainty of each pitch angle datum was assigned to the value shown on the abscissa, then an ensemble of 200 equilibria was reconstructed by VMEC with each experimental datum perturbed within its uncertainty. Two discharges were considered. The first, 68 257 (closed circles), is a typical TFTR supershot and has been analysed in Figs 2 to 8. The uncertainty in  $q(0)$  increases from 5.2% with the actual uncertainties to more than 30% for an uncertainty in the pitch angle measurement of  $1.25^\circ$ . The second discharge, 69 217 (closed triangles), is a low current,  $I_p = 500$  kA, high  $\beta_{pol} \approx 2$  discharge. No difficulty in reconstructing the high- $\beta_{pol}$  equilibrium was encountered because there was no plasma current ramp and this discharge did not develop a separatrix. The uncertainty in  $q(0)$  with the actual pitch angle uncertainties is acceptable, 7.1%, but rapidly increases to more than 40% for a pitch angle uncertainty of  $0.75^\circ$ . Not only does the accuracy decrease as the uncertainty rises, but the ability of the equilibrium code to converge also decreases for the high- $\beta_{pol}$  discharges. With the actual uncertainties, all of the equilibria converged. Only 70% of the code runs converged when the uncertainty was  $0.75^\circ$ .

In conclusion, an MSE polarimeter to measure the internal magnetic field direction at the plasma mid-plane has been installed on TFTR. When combined with the standard magnetics measurements and the equilibrium code VMEC, a powerful tool is available to analyse  $q$ , current density and magnetic shear profiles. This paper has focused on the uncertainty in the profile quantities based on experimental measurements. It is found that the computed value of  $q(0)$  is very robust with an uncertainty of 6% at the one standard deviation level. Likewise, the uncertainties in the  $q(R)$ , current density and shear profiles, which are important for transport and stability analyses, are also small. The primary source of uncertainty in the profiles determined by the equilibrium solver is the uncertainty of the magnetic field pitch angle measurements. However, without these measurements, a different, incorrect equilibrium would be computed. The small uncertainties actually achieved are due to the precision of the pitch angle and other measurements.

ACKNOWLEDGEMENTS

The authors would like to acknowledge many useful conversations with M. Mauel and R.V. Budny, the software support of J. Felt and the support of D.W. Johnson, K.M. Young, K.M. McGuire and M.C. Zarnstorff. This work was supported by USDOE Contract No. DE-AC02-76-CHO-3073.

REFERENCES

- [1] LEVINTON, F.M., et al., *Phys. Rev. Lett.* **63** (1989) 2060.
- [2] LEVINTON, F.M., et al., *Rev. Sci. Instrum.* **61** (1990) 2914.
- [3] LEVINTON, F.M., *Rev. Sci. Instrum.* **63** (1992) 5157.
- [4] WROBLEWSKI, D., LAO, L.L., *Rev. Sci. Instrum.* **63** (1992) 5140.
- [5] YAMADA, M., et al., *Phys. Plasmas* **1** (1994) 3269.
- [6] LAZZARO, E., MANTICA, P., *Plasma Phys. Control. Fusion* **30** (1988) 1735.
- [7] SOLTWISCH, H., *Plasma Phys. Control. Fusion* **34** (1992) 1669.
- [8] BLUM, J., et al., *Nucl. Fusion* **30** (1990) 1475.
- [9] LAO, L.L., et al., *Nucl. Fusion* **30** (1990) 1035.
- [10] ALLADIO, F., MICOZZI, P., *Nucl. Fusion* **35** (1995) 305.
- [11] HAWRYLUK, R.J., et al., in *Plasma Physics and Controlled Nuclear Fusion Research 1986* (Proc. 11th Int. Conf. Kyoto, 1986), Vol. 1, IAEA, Vienna (1987) 51.
- [12] COONROD, J., et al., *Rev. Sci. Instrum.* **56** (1985) 941.
- [13] HIRSHMAN, S.P., et al., *Phys. Plasmas* **1** (1994) 2277.
- [14] LEVINTON, F.M., et al., *Phys. Fluids B* **5** (1993) 2554.
- [15] CONDON, E.U., SHORTLY, G.H., *The Theory of Atomic Spectra*, Cambridge University Press, Cambridge (1963).
- [16] GOLDSTON, R.J., *J. Comp. Phys.* **43** (1981) 61.
- [17] HAWRYLUK, R.J., in *Physics of Plasmas Close to Thermonuclear Conditions* (Proc. Course Varenna, 1979), Vol. 1, CEC, Brussels (1980) 19.
- [18] LEVINTON, F.M., et al., *Phys. Rev. Lett.* **72** (1994) 2895.
- [19] KUZNETSOV, Yu.K., et al., *Nucl. Fusion* **26** (1986) 369.
- [20] LAO, L.L., et al., *Nucl. Fusion* **25** (1985) 1421.
- [21] SWAIN, D.W., NEILSON, G.H., *Nucl. Fusion* **22** (1982) 1015.
- [22] TAKAHASHI, H., et al., *Nucl. Fusion* **32** (1992) 815.
- [23] SABBAGH, S.A., *Bull. Am. Phys. Soc.* **38** (1993) 1984.
- [24] WOLF, R.C., et al., *Nucl. Fusion* **33** (1993) 1835.

(Manuscript received 3 July 1995

Final manuscript accepted 16 February 1996)